

MUSIC algorithm for RSSI-based DoA estimation on standard IEEE 802.11/802.15.x systems

MARCO PASSAFIUME, STEFANO MADDIO, ALESSANDRO CIDRONALI and GIANFRANCO MANES

University of Florence
Dept. of Information Engineering
Via di S.Marta, 3
Florence, Italy

marco.passafiume@unifi.it, stefano.maddio@unifi.it, alessandro.cidronali@unifi.it, gianfranco.manes@unifi.it

Abstract: Existing global positioning systems (GPS) applications are normally denied in indoor environments where, in spite of this limitation, a number of interesting applications are evolving into commercial products. At present, for indoor positioning, there are few cost-effective alternatives to GPS. One promising approach is based on the received signal strength indicator (RSSI) estimation, which is available in every IEEE standard compliant wireless transceiver, and includes useful information about the mutual positions between two position reference nodes. Extrapolating distance evaluation from RSSI is not reliable without the adoption of an accurate channel model [1],[2]. By using an anchor node/router with an array of directive antennas, it is possible to implement a spatial subdivision aimed at achieving an estimation of the direction of arrival (DoA) by evaluating the ratios between the single anchor's antennas, and thus independently of the channel characteristics. This approach makes use of already existing spectral-based DoA localization algorithms ([3],[4]), but all of them assume a real-time analysis of both the amplitude and the phase of the received signals. In this article, we demonstrate analytically the capability of the MUSIC algorithm [3] to elaborate only the RSSI readings. We also compare the DoA localization performance using the classical information set (i.e., amplitude and phase) versus the use of the RSSI set (obtained simply by reading transceiver standard registers). In conclusion, we introduce some fundamental array design principles for optimal MUSIC RSSI implementation, with a real implementation tracking test.

Key-Words: Indoor, positioning, tracking, WSN, DoA, RSSI, MUSIC, mobile devices, WiFi, Zigbee, Bluetooth

1 Introduction

In indoor device networks, a localization service is frequently provided using a constellation of routers (anchor nodes) in known positions; each of them estimates the DoA with respect to its angular reference system (as shown in Fig. 1).

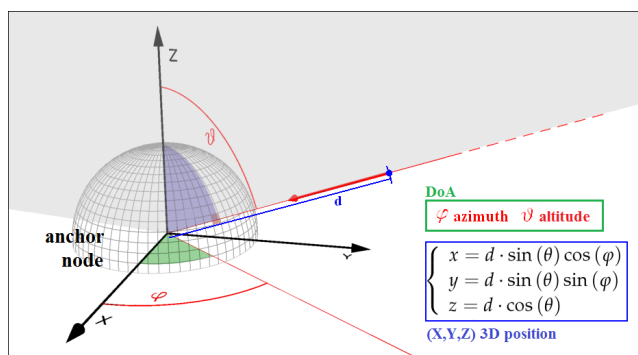


Figure 1: Anchor Node DoA reference system

For instance, in the configuration schematically shown

in Fig. 1, by using a triangulation approach, the knowledge of at least two pairs of angular coordinates (two DoAs, one for every anchor node) leads to a unique 3D spatial localization of a transmitter node; adding more anchors would improve the localization accuracy (cf. Fig. 2). To achieve the DoA estima-

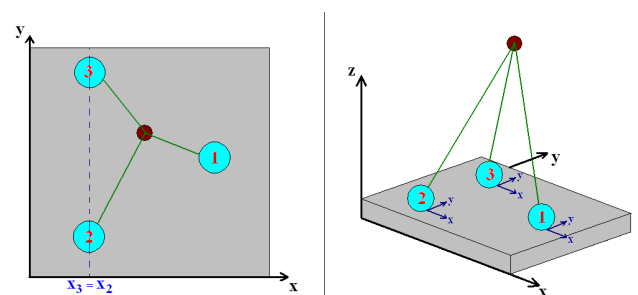


Figure 2: Multianchor localization

tion, independently of the adopted technique, an anchor node should allow some kind of spatial-diversity which enforces an almost biunivocal relationship between different DoAs and different data sets (defined

as a *steering vector*).

In such terms, the relative phases between the antennas of an array is the first type of suitable information available in a physical sampled data set.

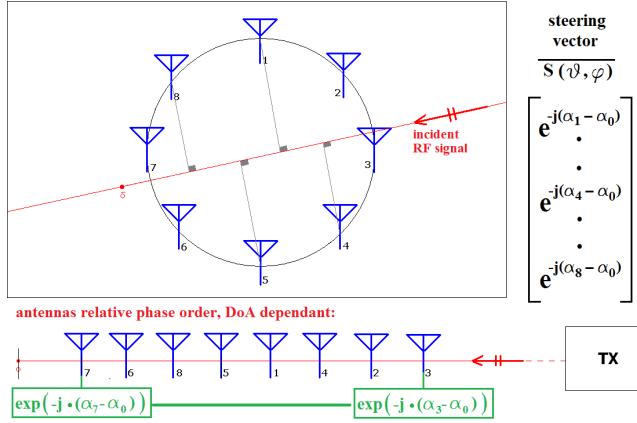


Figure 3: Simple TDOA approach example

In the equivalent time-domain approach represented in Fig. 3, the classical Time Difference of Arrival (TDOA) approach, the steering vector for an L -antenna circular array can be simply an L -dimensional vector containing the phase displacement terms for the received signals at each antenna compared to a given reference signal. More information could be added to the steering vector by sampling the incident power at each antenna of the array, adding in this way data about the relation between the DoA and the different angular gains of the antennas. It relevant to note that standard algorithm formulation expects as input data L -vectors of complex data, focusing the interest on the relative phase-terms.

1.1 Standard MUSIC algorithm

In this section, we review the MUSIC algorithm in its analytical form; a more detailed description is found in [3]. The MUSIC algorithm is defined as a *spectral-based* DoA localization algorithm: where spectral-based means that effective DoA identification is achieved by performing the membership analysis of a given measured/received data set, namely the *steering vector*, into a larger reference data set, which represents a reliable model for all possible received data sets associated to every expected DoA. Conventionally, the membership function resembles a *likelihood function* that for every reference steering vector returns a probabilistic index, which expresses the degree of relationship to the reference one. Following the formal MUSIC formulation in [3], the obtained steering vector for an L -antenna array becomes an L -element vector of complex samplings of signal ampli-

tudes/phases.

In a generic M -signals case, the steering vector will be somewhat as in Eq. 1.

$$\bar{\mathbf{x}}(t) = \sum_{j=1}^M \underbrace{\begin{pmatrix} g_1(\theta_j, \varphi_j) e^{-j\varphi_{1j}} \\ g_2(\theta_j, \varphi_j) e^{-j\varphi_{2j}} \\ \vdots \\ g_L(\theta_j, \varphi_j) e^{-j\varphi_{Lj}} \end{pmatrix}}_{\bar{\mathbf{m}}(\theta_j, \varphi_j) = \bar{\mathbf{m}}_j} s_j(t) + \bar{\mathbf{n}}(t)$$

with $(\theta_j, \varphi_j) = j$ -th signal DoA (1)

In Eq. 1, the overall observation noise, which represents the measurement noise plus radio noise over the linkpath, is modeled by $\bar{\mathbf{n}}(t)$ vector with L elements. As in [3], every $n_i(t)$ term can be considered as AWGN noise, with zero mean, with known variance, and impulsive autocorrelation (producing $n_i(t)$ statistically independent terms).

Each $\bar{\mathbf{m}}_j$ vector corresponds to a singular steering vector for the given j th signal (associated to the j th DoA): every antenna component is defined with a $g_i(\theta_j, \varphi_j)$ term modeling the antenna's directional linear gain and a phase delay which represents the relative antenna phase displacement (both terms dependent on the signal DoA, as in Fig. 3, with improved gain-DoA dependence).

Envisioning the implementation of a localization service within a common network of devices, effective communication should be achieved using a protocol of channel multiplexing (like TDM or FDM) also to minimizing communication interferences, so considering the localization of only one signal $s_1(t)$ is a realistic restriction.

Following the standard MUSIC implementation [3], from $\bar{\mathbf{x}}(t)$, an \mathbf{R} autocorrelation matrix is produced (Eq. 2).

$$\begin{aligned} \mathbf{R}_{ij} &= E\{x_i(t)x_j^*(t)\} = \\ &= m_i(\theta_T, \varphi_T) m_j^*(\theta_T, \varphi_T) \cdot E\{s_1^2(t)\} + \\ &+ E\{n_i(t)n_j^*(t)\} + \\ &+ \frac{m_i(\theta_T, \varphi_T) \cdot E\{s_1(t)n_i(t)\}}{m_j^*(\theta_T, \varphi_T) \cdot E\{s_1(t)n_j(t)\}} = \\ &= m_i m_j^* P + \begin{cases} N \leftarrow i = j \\ 0 \leftarrow i \neq j \end{cases} \end{aligned} \quad (2)$$

Overall, the \mathbf{R} matrix can be seen as a linear combination of two principal submatrices (Eq. 3), presenting a maximum rank equal to L (equal to the number of antennas) because adding with the identity matrix

generated by uncorrelated noise terms (Eq. 2).

$$\mathbf{R} = \underbrace{\mathbf{M}(\theta_T, \varphi_T) \cdot P}_{\text{rank}=1} + \underbrace{\mathbf{I} \cdot N}_{\text{rank}=L} \quad (3)$$

Because \mathbf{R} has maximal rank, it completely defines a \mathbf{C}^L vector space: consequently every basis of eigenvectors defines a complete basis for the \mathbf{C}^L space. It is easy to demonstrate that in Eq. 3, \mathbf{R}_S has unitary rank with only one eigenvector equal to $P \cdot \bar{\mathbf{m}}(\theta_T, \varphi_T)$, with eigenvalue $\lambda_M = \|\bar{\mathbf{m}}(\theta_T, \varphi_T)\|^2 P$, that turns out parallel to the characteristic DoA steering vector in the reference data set (Fig. 4). This fact is demonstrated in [3], but the result could be achieved also using a standard mathematical analysis software. As

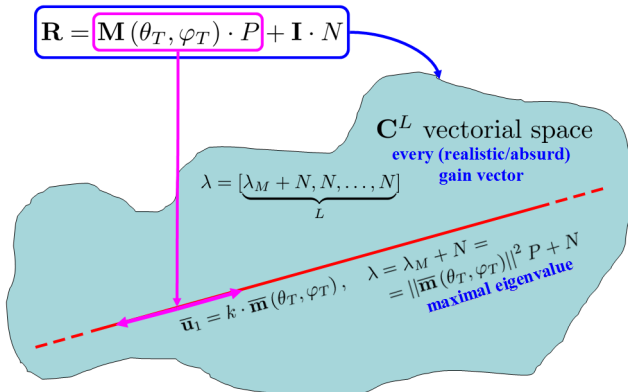


Figure 4: Vectorial space subdivision

the \mathbf{R}_N matrix term has maximum rank, extracting a full basis of eigenvectors for \mathbf{R} with their corresponding eigenvalues, and observing that \mathbf{R}_N will present a set of L equal eigenvalues (equal to N , as in Eq. 2), it is clear that the signal eigenvector will be that one associated to the maximum extracted eigenvalue.

By a calculation, all the global eigenvectors of \mathbf{R} (in order of the magnitude of the eigenvalue) are shown in Eq. 4:

$$\lambda_1 = \|\bar{\mathbf{m}}(\theta_T, \varphi_T)\|^2 \cdot P + N \Rightarrow \bar{\mathbf{u}}_1 = \frac{\bar{\mathbf{m}}(\theta_T, \varphi_T)}{m_L}$$

$$\lambda_{2...L} = N \Rightarrow \Rightarrow \left(\begin{array}{c} -\frac{m_2}{m_1} \\ 1 \\ \vdots \\ 0 \\ 0 \end{array} \right), \left(\begin{array}{c} -\frac{m_3}{m_1} \\ 0 \\ 1 \\ \vdots \\ 0 \end{array} \right), \dots, \left(\begin{array}{c} -\frac{m_L}{m_1} \\ 0 \\ 0 \\ \vdots \\ 1 \end{array} \right) \quad (4)$$

$\bar{\mathbf{u}}_2 \qquad \bar{\mathbf{u}}_3 \qquad \bar{\mathbf{u}}_L$

From 4 it is important to see how all *noise eigenvectors* turn out to be fully orthogonal only with the right DoA steering vector $\bar{\mathbf{m}}(\theta_T, \varphi_T) = [m_1, m_2, \dots, m_L]^T$.

Consequently, if all reference steering vectors will be projected onto \mathbf{R} , only the right DoA one will give a *null projection* onto the subspace defined by the *noise eigenvectors*: for this, the subspace defined by the noise eigenvectors could be defined as the *subspace of absent signals DoA*.

This fact is fundamental, because verifying when the reference DoA steering vector is parallel to the obtained DoA isn't immediate (the need to have the 'maximum' projection onto the *received signal DoA steering vector subspace*), the orthogonal property is stronger and faster to implement.

Obtaining a *subspace of absent signals DoA* definition matrix \mathbf{U}_N as shown in Eq. 5, which contains all the eigenvectors for the *subspace of absent signals DoA steering vectors*—extracted using techniques like the Singular Value Decomposition algorithm [5], it becomes possible to define a *projection function* for a steering vector onto its defined space.

$$\mathbf{U}_N = \langle \bar{\mathbf{u}}_2 | \bar{\mathbf{u}}_3 | \dots | \bar{\mathbf{u}}_L \rangle = \quad (5)$$

$$= \left(\begin{array}{c|c|c|c} -\frac{m_2}{m_1} & -\frac{m_3}{m_1} & & -\frac{m_L}{m_1} \\ 1 & 0 & & 0 \\ \vdots & 1 & \dots & 0 \\ 0 & \vdots & & \vdots \\ 0 & 0 & & 1 \end{array} \right)$$

$L \text{ rows} \times (L-1) \text{ columns}$

Given the \mathbf{U}_N space definition matrix and \mathbf{U}_N^H its Hermitian, the normalized projection function of every reference *steering vector* $\bar{\mathbf{m}}(\theta, \varphi)$ onto the *absent space* could be defined as in Eq. 6.

$$p_m(\theta, \varphi) = \frac{\|\mathbf{U}_N^H \cdot \bar{\mathbf{m}}(\theta, \varphi)\|}{\underbrace{\|\bar{\mathbf{m}}(\theta, \varphi)\|}_{\text{normalized projection}}} \quad (6)$$

In Eq. 6, a normalization factor with respect to the reference input steering-vector module is placed. This term is required because there could exist disadvantaged DoAs with associated steering vectors having small components tending to 0: when the signal reaches the array over one of these DoAs, the projection onto \mathbf{U}_N could be reduced a lot also for the wrong DoA's reference steering vectors. In an ideal scenario, these wrong DoAs would give a non-zero (but small, tending towards zero) projection, so a correct identification of the minimum point could

be achieved: this problem becomes severe when the algorithm has to be implemented in a finite precision computing unit, where a zero truncation will be performed for values under the minimal data resolution, no longer yielding only one minimum projection point, but more than one, leaving an indetermination problem for DoAs with weaker array gains.

The MUSIC spectrum is defined as the maximum corresponding to the best estimated DoA. The *projection function* is defined onto the space of DoAs with precomputed *steering vectors* in the reference data set (on an \mathbf{R}^2 space), and has the minimum value for the best estimated DoA: so, the effective MUSIC-spectrum function is shown in Eq. 7—equivalent to the function shown in [3].

$$P_m(\theta, \varphi) = \frac{1}{p_m(\theta, \varphi)} = \frac{\|\bar{\mathbf{m}}(\theta, \varphi)\|}{\|\mathbf{U}_N^H \cdot \bar{\mathbf{m}}(\theta, \varphi)\|} \quad (7)$$

2 Applying RSSI measurements to MUSIC

IN the preceding, the theoretical MUSIC algorithm has been reviewed. In the literature, localization accuracy analyses (CRB-like) are performed only for direct physical signal analysis [4], because following the standard definition in [3], there is added a measure-noise term following the AWGN noise definition, which is reliable only for physical signal observations. Also, the projection's capability of rejecting valid steering vector onto the *absent signal subspace* is stronger when the the condition of orthonormality between two different DoA steering vectors is stronger (minimizing their scalar product), and this condition is helped with complex steering vectors.

Below, an analytical application model for the RSSI-values MUSIC application will be suggested, and in that way, there will be presented some conditions for assuring the right MUSIC execution with simple RSSI measurements.

2.1 Analytical application model

Eq. 8 gives the standard projection operator between the obtained steering vector $\bar{\mathbf{v}}$ and the reference one $\bar{\mathbf{m}}(\theta, \varphi)$.

$$\begin{aligned} \|\bar{\mathbf{v}}^* \cdot \bar{\mathbf{m}}(\theta, \varphi)\| &= \left| \sum_{i=1}^L v_i^* m_i(\theta, \varphi) \right| = \quad (8) \\ &= \left| \underbrace{\sum_{i=1}^L \left(g_{i(\theta_T, \varphi_T)} e^{j \varphi_i(\theta_T, \varphi_T)} \right)}_{\text{obtained steering vector}} \underbrace{\left(g_i(\theta, \varphi) e^{-j \varphi_i(\theta, \varphi)} \right)}_{\text{ref. steering vector}} \right| \end{aligned}$$

From Eq. 8, it is clear that with same antenna gains ($g_{i(\theta_T, \varphi_T)} = g_i(\theta, \varphi)$) the projection is maximized (and so the MUSIC-spectrum is maximized) if

$$\forall i, \varphi_i(\theta_T, \varphi_T) = \varphi_i(\theta, \varphi). \quad (9)$$

Without using phase displacement information, the question is whether the projection maximization is achieved only for the right reference steering vector, associated to the right DoA. This analysis considers the acquisition of the RSSI values.

For IEEE wireless standards, the transceiver RSSI parameter is a number that is computed during the demodulation process, and it is given by an average over a variable-length window of symbols of cross-correlation peak levels between the demodulated RF base-band signal and the symbol reference signal sequences (for spread-spectrum modulated signals). It can be roughly correlated with the dB level of the power signal detected at the radio interface in the input to the transceiver, weighted for a calibration constant (not necessarily known). Due to the nature of its evaluation, the RSSI parameter itself presents a measure error that could be modeled to a first approximation like an added AWGN noise: so, for the i th antenna, the RSSI detected value is something like $X_i(t) = RSSI_i + \Delta R_i(t)$, with $\Delta R_i(t)$ the AWGN measure noise.

Applying MUSIC[3], for a given steering vector the autocorrelation matrix \mathbf{R} has to be created: the correlation value must tend to 0 when the i th good signal received from antenna i is correlated with the the j th null signal received from the blind antenna j , so it is necessary to transform the acquired values into linear equivalent ones. So, with measure noise (within-signal noise can also be modeled, which causes an alteration of the RSSI readings), every term of the steering vector $\bar{\mathbf{x}}$ becomes like that in Eq. 10.

$$\begin{aligned} x_i(\theta_T, \varphi_T) &= K_0 \cdot 10^{\frac{\overbrace{(RSSI_i + \Delta R_i(t))}^{x_i}}{10}} = \quad (10) \\ &= K_0 [P \cdot N_i(t) \cdot g_{i(\theta_T, \varphi_T)}] \end{aligned}$$

with $P = E\{s_1^2(t)\}$ = incident signal power

Note that in comparison with Eq. 1, data sampling over time has lost its natural time-dependency: now, with a static signal DoA, antenna sampling over time will result in a constant data set with minor changes due to measure noise, but not related to the intrinsic signal shape.

Transforming the RSSI units to linear ones, a catastrophic effect is caused by the generation of the i th coefficient of the N_i due to the linear conversion from

RSSI noise ΔR_i : during the projection of the acquired steering vector over the reference data set, Eq. 8 will be changed to Eq. 11, causing dramatic alterations of the norms of the projections onto the possible DoA steering vectors subspace, with consequent dramatic mismatches with the DoA identification, so some conditions on the RSSI measurements have to be imposed.

$$\|\bar{\mathbf{v}}^* \cdot \bar{\mathbf{m}}(\theta, \varphi)\| = \sum_{i=1}^L N_i(t) [g_{i(\theta_T, \varphi_T)} g_{i(\theta, \varphi)}] \quad (11)$$

It will be investigated how the MUSIC \mathbf{R} autocorrelation matrix will be altered, with related eigenvectors. Due to the time-variant nature of the RSSI measurement noise term $\Delta R_i(t)$, the steering vector terms will necessarily have the form in Eq. 12, removing the K_0 coefficient of Eq. 10 thanks to the MUSIC-spectrum projection normalization (Eq. 7).

$$x_{i(\theta_T, \varphi_T)}(t) = P \cdot N_i(t) \cdot g_{i(\theta_T, \varphi_T)} \quad (12)$$

with $N_i(t) = 10^{\frac{\Delta R_i(t)}{10}}$.

Putting Eq. 12 directly into Eq. 2 does not lead to valid results (the subspace separation can not be achieved), because in the new $x_{i(\theta_T, \varphi_T)}$ terms, there does not exist a linear separation between the signal terms and noise terms.

To get a result comparable with Eq. 2 and then to Eq. 3, with the ability to make an *absent DoA signal vectorial subspace*, some evaluation of the $N_i(t)$ term must be done. Considering $\Delta R_i(t)$ as an unknown statistical variable that comes from an analog-digital process, it will be assigned an uniform zero-mean statistic: making a worst case assumption, the linear units $N_i(t)$ term will a uniformly distributed variable with limits coming from the $\Delta R_i(t)$ ones. The statistical properties of $N_i(t)$ and $\Delta R_i(t)$ are given in Eq. 13.

$$\Delta R_i(t) \in [-\epsilon_{MAX}, \epsilon_{MAX}] \Rightarrow \quad (13)$$

$$\Rightarrow N_i(t) \in \left[10^{\frac{-\epsilon_{MAX}}{10}}, 10^{\frac{\epsilon_{MAX}}{10}} \right]$$

$$\Delta R_i(t) \begin{cases} \mu_R = 0 \\ \sigma_R^2 = \frac{\epsilon_{MAX}^2}{3} \end{cases}$$

$$N_i(t) \begin{cases} \mu_N = \frac{10^{\frac{\epsilon_{MAX}}{10}} + 10^{\frac{-\epsilon_{MAX}}{10}}}{2} \\ \sigma_N^2 = \frac{1}{12} \left(10^{\frac{\epsilon_{MAX}}{10}} - 10^{\frac{-\epsilon_{MAX}}{10}} \right)^2 \end{cases}$$

Following Eq. 13, $N_i(t)$ factor can be written as

$$N_i(t) = \mu_N + n_i(t) \leftarrow \begin{cases} \mu = 0 \\ \sigma = \sigma_N \end{cases} \quad (14)$$

$$\text{with } \begin{cases} E\{n_i^2(t)\} = \sigma_N^2 & \text{equivalent noise power} \\ E\{n_i(t) \cdot n_i(t - \tau)\} = 0 & \text{if } \tau \neq 0 \end{cases}$$

where $n_i(t)$ term is not an AWGN noise, but shares with it its impulsive autocorrelation (meaning that the $n_i(t)$ and $n_j(t)$ terms are statistically independent). The μ_N and σ_N terms are related to ϵ_{MAX} (equal to the maximum transceiver given RSSI deviation) following the plots in Fig. 5. Using new linear formula-

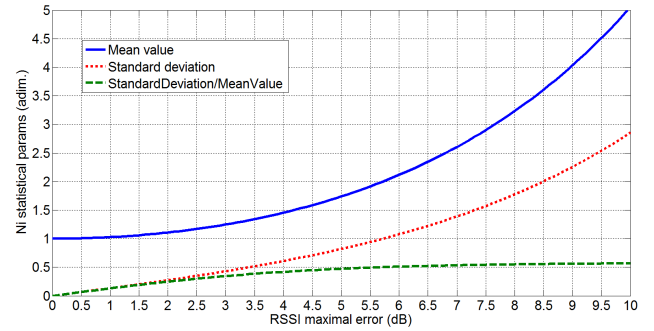


Figure 5: $N_i(t)$ mean and variance, with respect to ϵ_{max}

tion for $N_i(t)$, it is possible to rearrange Eq. 2. Single $x_i(t)$ term become as shown in Eq. 15.

$$x_{i(\theta_T, \varphi_T)}(t) = \overbrace{[\mu_N + n_i(t)]}^{N_i(t)} P \cdot g_{i(\theta_T, \varphi_T)} = \quad (15)$$

$$= \mu_N P \cdot g_{i(\theta_T, \varphi_T)} + n_i(t) P \cdot g_{i(\theta_T, \varphi_T)}$$

So, using the noise properties as in Eq. 14, the generic \mathbf{R}_{ij} term results as in Eq. 16, where $\bar{\mathbf{g}}(\theta_T, \varphi_T) = \bar{\mathbf{m}}(\theta_T, \varphi_T)$, because of the lack of phase displacement complex terms in Eq. 1.

$$\mathbf{R}_{ij} = E\{x_i(t)x_j^*(t)\} = \quad (16)$$

$$= g_{i(\theta_T, \varphi_T)} g_{j(\theta_T, \varphi_T)} P^2 (\mu_N^2 + E\{n_i(t)n_j^*(t)\}) +$$

$$+ \cancel{g_{i(\theta_T, \varphi_T)} P \cdot E\{n_i(t)\}} +$$

$$+ \cancel{g_{j(\theta_T, \varphi_T)} P \cdot E\{n_j(t)\}} =$$

$$= \underbrace{(\mu_N P)^2 g_{iT} g_{jT}}_{\mathbf{R}_S} + \underbrace{\begin{cases} (\sigma_N P)^2 g_{iT}^2 & \leftarrow i = j \\ 0 & \leftarrow i \neq j \end{cases}}_{\mathbf{R}_N}$$

Comparing Eq. 16 with Eq. 2, although the correspondence between the \mathbf{R}_S terms is clear, the structure of the \mathbf{R}_N submatrix is greatly changed, becoming directly dependent on the DoA because of the presence

of the $g_i^2(\theta_T, \varphi_T)$ terms. The distortion effect onto the DoA subspaces is directly related with the relative weight of \mathbf{R}_N in the linear combination (as in Eq. 3), so the ratio between \mathbf{R}_S and \mathbf{R}_N will be directly related to the MUSIC estimation error. Applying an SVD decomposition [5], the submatrix weights are defined as in Eq. 17.

$$\mathbf{M}_{\text{weight}} = \det(\mathbf{M}) = \sum_{i=1}^L \lambda_i \cdot \|\bar{\mathbf{v}}_i\|^2$$

where λ_i is the i th eigenvalue
 $\bar{\mathbf{v}}_i$ is the i th eigenvector
 L is the matrix order (17)

For standard MUSIC, the results are

$$\mathbf{R}_S \text{ weight} = P \cdot \|\bar{\mathbf{m}}(\theta_T, \varphi_T)\|^4 = P \cdot \left(\sum_{i=1}^L g_{iT}^2 \right)^2$$

$$\mathbf{R}_N = \underbrace{N \cdot \mathbf{I}}_{\text{rank}=L} \Rightarrow \boxed{\mathbf{R}_N \text{ weight} = N \cdot L} \quad (18)$$

For RSSI MUSIC:

$$\mathbf{R}_S \text{ weight} = (\mu_N P)^2 \|\bar{\mathbf{m}}\|^4 = (\mu_N P)^2 \cdot \left(\sum_{i=1}^L g_{iT}^2 \right)^2$$

$$\mathbf{R}_N = (\sigma_N P)^2 \cdot \begin{pmatrix} g_{1T}^2 & 0 & 0 \\ & \ddots & \\ 0 & 0 & g_{LT}^2 \end{pmatrix}$$

$$\boxed{\mathbf{R}_N \text{ weight} = (\sigma_N P)^2 \cdot \left(\sum_{i=1}^L g_{iT}^2 \right)} \quad (19)$$

The quality of the MUSIC estimation (interpreted as the proximity between the hypothesized and the real signal DoA) is directly related to ratio of the weights of the submatrices, so a quality factor is defined as in Eq. 20.

$$Q_{\text{FACTOR}} = \left(\frac{\mathbf{R}_S \text{ weight}}{\mathbf{R}_N \text{ weight}} \right) \underbrace{\left(\sum_{i=1}^L g_{iT}^2 \right)^{-1}}_{(*) \text{ DoA weight}} \quad (20)$$

Eq. 21 shows the ‘quality factors’ for the standard and the RSSI MUSIC implementations.

$$\text{std. MUSIC} \Rightarrow \boxed{Q_{STD} = \frac{P}{NL} \left(\sum_{i=1}^L g_{iT}^2 \right) \leq \frac{P}{N}}$$

$$\text{RSSI MUSIC} \Rightarrow Q_{RSSI} = \left(\frac{\mu_N}{\sigma_N} \right)^2 \approx \frac{1}{\sigma_N^2} \quad (21)$$

Note that in Eqs. 18–19, the \mathbf{R}_S weights are multiplied by a DoA-related term that can be normalized (*) (it represents the dependence of the accuracy of the DoA in relation to the array structure, and is normalized by the *MUSIC spectrum* normalization as in Eq. 7).

Comparing the ratios in Eq. 21, it can be observed that for the RSSI implementation, the quality factor depends directly on the quality of the RSSI evaluation, while for the standard implementation, there remains a DoA dependency due to the effective physical SNR alteration when different DoAs lead to different signal antenna gains. For RSSI, this behaviour is mended by the RSSI evaluation correlation mechanism.

Using Eq. 13, the quality factor for the RSSI implementation can be directly related to the maximal RSSI evaluation error ϵ_{MAX} , as below.

$$Q_{RSSI} = 3 \cdot \left(\frac{10^{\frac{\epsilon_{MAX}}{10}} + 10^{-\frac{\epsilon_{MAX}}{10}}}{10^{\frac{\epsilon_{MAX}}{10}} - 10^{-\frac{\epsilon_{MAX}}{10}}} \right)^2 \quad (22)$$

Because for the standard implementation, the *quality factor* is directly related with the physical SNR, it is possible to make a direct comparison of the RSSI transceiver uncertainty with the equivalent physical signal state. Fig. 6 shows the trend of Eq. 22.

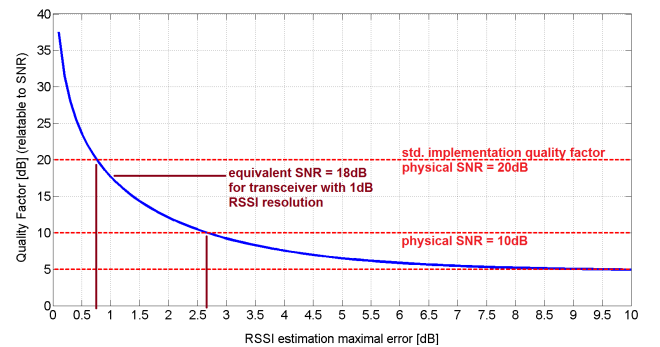


Figure 6: MUSIC RSSI implementation Q-Factor

2.2 Design principles for the array structure

Before evaluating MUSIC RSSI vs the standard implementation, some further considerations about the physical constraints on the antenna arrays must be made.

A simple condition for a good phaseless RSSI MUSIC implementation is a direct consequence of the vectorial projection structure. In Eq. 11, there was shown

the standard RSSI projection norm of the received real-term steering vector $\bar{\mathbf{g}}(\theta_T, \varphi_T)$ onto the reference steering vector $\bar{\mathbf{g}}(\theta, \varphi)$: ignoring the N_i noise term, the projection norm is given by Eq. 23.

$$\|\bar{\mathbf{v}}^* \cdot \bar{\mathbf{m}}(\theta, \varphi)\| = \sum_{i=1}^L [g_{i(\theta_T, \varphi_T)} \cdot g_i(\theta, \varphi)] \quad (23)$$

A DoA mismatch happens when there exists a DoA $(\theta_E, \varphi_E) \neq (\theta_T, \varphi_T)$ for which

$$\|\bar{\mathbf{v}}^* \cdot \bar{\mathbf{m}}(\theta_E, \varphi_E)\| \geq \|\bar{\mathbf{v}}^* \cdot \bar{\mathbf{m}}(\theta_T, \varphi_T)\| \quad \text{or rather}$$

$$\sum_{i=1}^L [g_{i(\theta_T, \varphi_T)} g_{i(\theta_E, \varphi_E)}] \geq \sum_{i=1}^L [g_{i(\theta_T, \varphi_T)}]^2$$

Note that this is surely verified if the *sufficient condition* in Eq. 24 is true.

$$\forall i : g_{i(\theta_E, \varphi_E)} \geq g_{i(\theta_T, \varphi_T)} \quad (24)$$

As a result, a *necessary condition* for the design of the array structure is given: Eq. 24 says that a DoA (θ_T, φ_T) will be *surely* misunderstood with the DoA (θ_E, φ_E) when it has all RSSI related gain terms strictly less than or equal to the corresponding antenna RSSI gain terms related with the wrong DoA.

Avoiding this condition, for working with phase-less RSSI MUSIC it becomes mandatory to use arrays with strong spatial diversity in their antenna gains, using, if possible, directive antennas oriented differently, as shown in Fig. 7. A valid array structure is presented in [9],[10]: in [12], the impact of the array geometry on the RSSI DoA estimation is investigated. More detailed considerations could be made by ana-

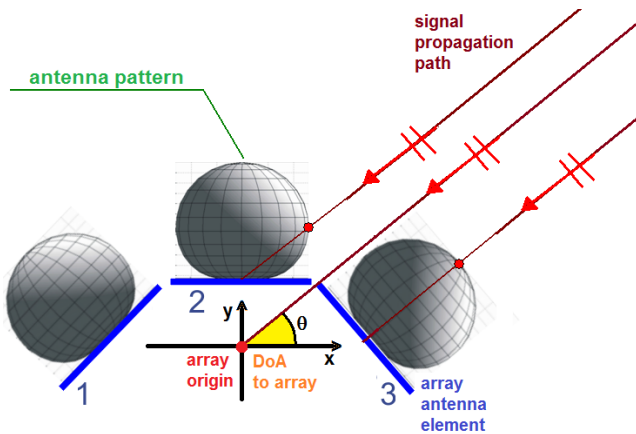


Figure 7: Example of array structure for RSSI MUSIC

lyzing effective MUSIC projection computation: following Eq. 5, the projection norm of $\bar{\mathbf{g}}(\theta, \varphi)$ on the

\mathbf{U}_N space is shown below. It is clear that for $(\theta, \varphi) \rightarrow (\theta_T, \varphi_T)$, the projection of $\bar{\mathbf{g}}$ onto \mathbf{U}_N goes to 0.

$$\begin{aligned} G_N(\theta, \varphi) &= \|\mathbf{U}_N^H \cdot \bar{\mathbf{g}}(\theta, \varphi)\| = \dots \quad (25) \\ &= \sqrt{\sum_{i=2}^L \left| \underbrace{g_i(\theta, \varphi) - \frac{g_i(\theta_T, \varphi_T)}{g_1(\theta_T, \varphi_T)} g_1(\theta, \varphi)}_{\bar{\mathbf{g}}(\theta, \varphi) \cdot \bar{\mathbf{u}}_i} \right|^2} = \\ &= |g_1(\theta, \varphi)| \sqrt{\sum_{i=2}^L \left| \frac{g_i(\theta, \varphi)}{g_1(\theta, \varphi)} - \frac{g_i(\theta_T, \varphi_T)}{g_1(\theta_T, \varphi_T)} \right|^2} \end{aligned}$$

So, applying Eq. 25 in Eq. 7, an equivalent form for the MUSIC pseudospectrum function is obtained (Eq. 26).

$$\begin{aligned} \text{MUSIC spectrum } P_m(\theta, \varphi) &= \frac{\|\bar{\mathbf{g}}(\theta, \varphi)\|}{G_N(\theta, \varphi)} \\ P_m(\theta, \varphi) &= \frac{1 + \sum_{i=2}^L \left| \frac{g_i(\theta, \varphi)}{g_1(\theta, \varphi)} \right|^2}{\sqrt{\sum_{i=2}^L \left| \frac{g_i(\theta, \varphi)}{g_1(\theta, \varphi)} - \frac{g_i(\theta_T, \varphi_T)}{g_1(\theta_T, \varphi_T)} \right|^2}} \quad (26) \end{aligned}$$

Eq. 26 shows better the relation between the performance of the MUSIC pseudospectrum and the correlation between the array antenna gains. Real DoA information is carried only by the ratios between the antenna gains: hence, it is clear that the key to good physical array design for using MUSIC without phase-information is improving the range subdivision of the DoAs, covering the overall range of DoAs with as many array elements as possible.

Furthermore, in contrast to the requirements of standard phased implementations, the requirement of maximizing the ratio differentiation between the DoAs dramatically increases the need to use high directivity antennas: in the next section, a case analysis will be performed. It is important to remember that a compromise between antenna directivity and the number of array elements must be achieved, because it is necessary to realize good gain coverage of the complete range of DoAs: DoAs with small array gains will show an equivalent lack of spatial gain differentiation, while the RSSI detection error will alter dramatically with changes in the ratios between the gains.

3 Comparison of simulation results

An approximate CRB comparison between the implementations will be shown. It simulates a 1D DoA identification placing a planar array with an incident RF 2.45GHz ($\lambda \approx 12$ cm) signal coming from its frontal horizon (DoAs in $[-\frac{\pi}{2}, \frac{\pi}{2}]$): the

CRB index approximately evaluates the mean of the standard deviations of the DoA estimations, for every DoA in domain, over 50 MUSIC executions for each implementation over a noisy obtained data set of 50 samples.

Following the requirements proposed in 2.2, structures for arrays will be different between the phase and phase-less RSSI MUSIC implementations, to optimize the functional conditions. For phased MUSIC, an Uniform Linear Array (ULA) is configured, maximizing the center-of-phase interdistances for maximizing the phase-displacement differentiation between the DoAs. Instead, for the phase-less MUSIC, an Uniform Circular Array (UCA) is placed (similar to 8) to guarantee the maximal DoA antenna gain diversification (as in [12]): for both cases, the antenna gains follow a cardioid directive shape (Fig. 9) as in [6], with a front-to-back ratio of 30 dB. Note

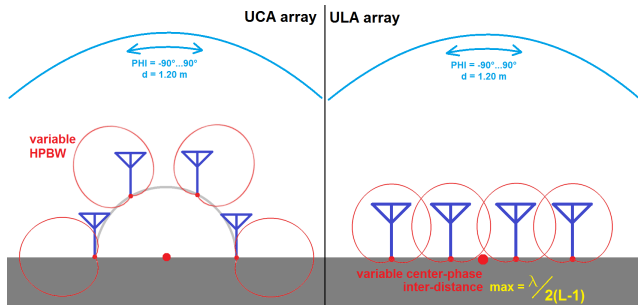


Figure 8: Simulated array structures

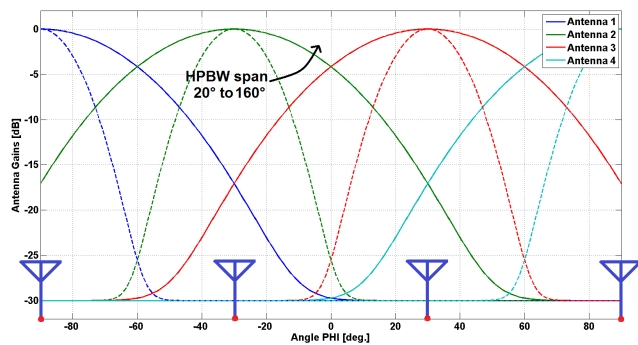


Figure 9: UCA antenna gains versus DoA

that for ULA configuration array lengths in the range of $d \in (0, \frac{\lambda}{2}] \Rightarrow \Delta d_{max} = \frac{\lambda}{2(L-1)}$ allow preserving coherent phase information in the face of every possible incident DoA, also with real phase-detector detection ambiguity between phases in the ranges $[-\pi, 0]$ and $[0, \pi]$. CRBs are evaluated for different array configurations (varying antenna HPBWs for UCA, array interdistances for ULA) and for different Q-Factors. In order to make a valid comparison, for both implementations, the x -axis plot is related to the

maximum RSSI deviation: for UCAs, the Q-Factor is known (Eq. 21), and for ULAs, the SNR is directly set equal to the UCA's Q-Factors (calculated with Eq. 22) for every case.

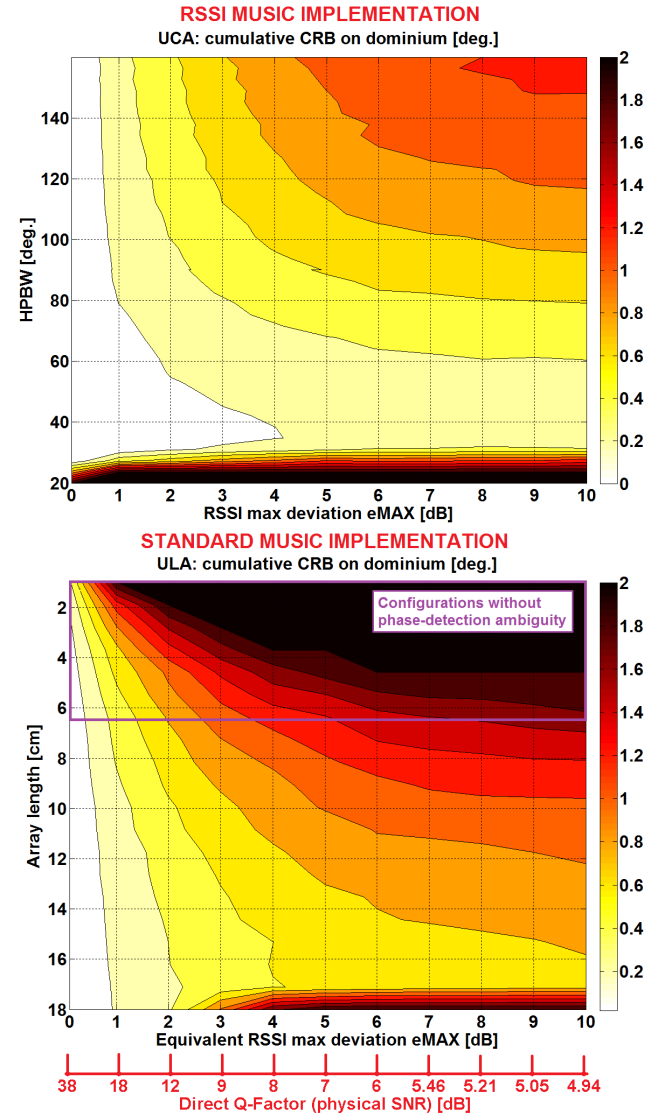


Figure 10: CRB-like estimation for UCAs (a) and ULAs (b) configs, versus equivalent RSSI max error

As shown in Fig. 10, the MUSIC RSSI implementation shows a more reliable behaviour: this is due to the presence in the amplitude/phase acquisitions of noise contributions over both measured variables, increasing the obtained steering vector distortion.

A fundamental hypothesis is that RSSI alteration should be under ϵ_{MAX} due to noise effects at lower SNRs, meaning that RSSI differences between antennas must preserve coherent information about the ratios between the directional antenna gains. Digital modulation protects the RSSI evaluations

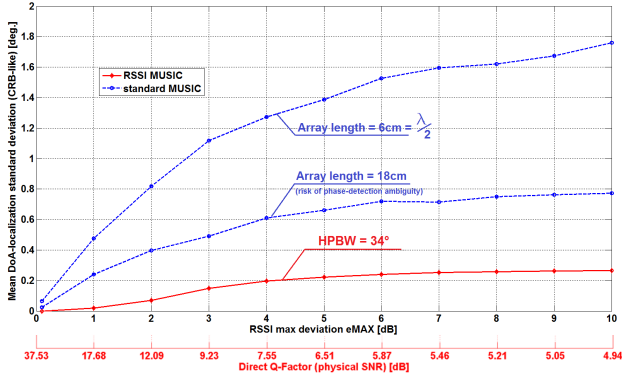


Figure 11: CRB-like vs measurement noise comparison between RSSI/standard MUSIC implementations for UCA/ULA best configurations

from being skewed by channel noise (by using spread spectrum and advanced decoding correlation techniques [13], [14]), so in a clear environment it is right to consider RSSI measurements as more reliable than the direct signal evaluation approach: consequently, the RSSI MUSIC implementation is preferable for implementing low-cost DoA identification systems, as in [11].

4 Real implementation testing

For showing the architectural and functionality improvement given by an RSSI implementation of MUSIC for a DoA localization system, the results of some angular localization tests will be given for an actually implemented architecture ([11]) which is based on standard off-the-shelf components and uses the standard 802.15.4 IEEE protocol for communications.

The system presented in [11] meets the strict requirement of interoperability with standard mobile nodes operating with 802.15.4: this is mandatory for the implementation of a standard radio transceiver according to the 802.15.4 IEEE standard, and without which, a cost-effective system implementation of some advanced phase-displacement detectors over antennas of array would be unthinkable.

The major emphasis is given to planar antenna design, to obtain predictable directive RSSI antenna gains (so the ideal gains model can be used as a good *reference data set* – Fig. 12): known antenna parameters also avoid the problems shown in [15]. The localizing anchor node consists in an array of 8 highly directive left-handed circular polarized antennas (presented in [7],[8]), uniformly disposed over a spherical space around the node (Fig. 12): the array is connected to a TI CC2430 RF transceiver (with RSSI maximal detection error $\epsilon_{MAX} \approx 1dB$ – [13]) through an 8-to-1

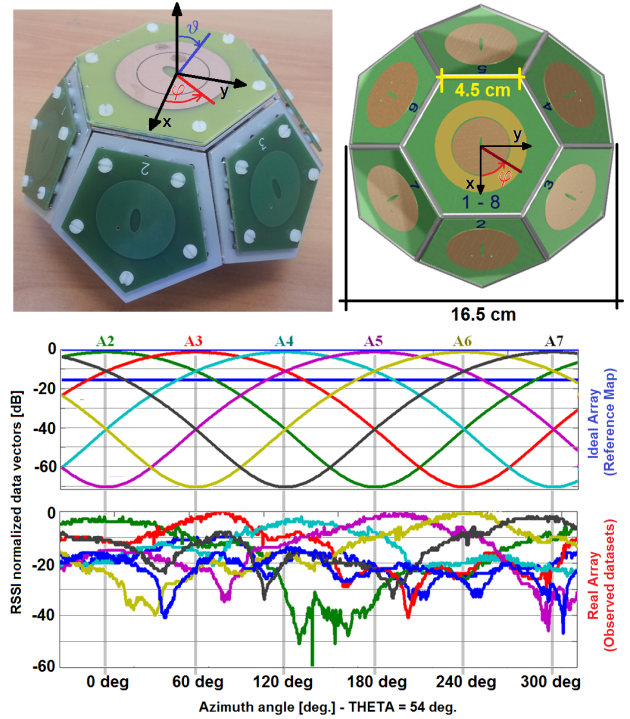


Figure 12: RSSI/DoA localization system hardware(a), azimuthal antennas RSSI data vectors(b)

RF switch which realizes a time division multiplexing of the transceiver RF link between the different array elements.

Despite this, the localizing anchor node is placed as a singular network device, and a special firmware makes the necessary adjustments for supplying the 802.15.4 compatibility to the device: the whole anchor-node has an IP address and the RSSI data vectors are obtained by a computer through a standard ethernet interface. Note that the RSSI measurements are embedded with standard mobile communicating nodes data, so during the localization, data communication is also provided.

In these tests, the mobile node is intended to be a standard 802.15.4 IEEE transceiver connected to a coupled left-handed circular polarized antenna.

DoA localizations are performed over a tracking path at a distance of 120 cm, using the DoA reference system shown in Fig. 1. The mobile node is placed at an orientation of $\theta = 54^\circ$, making the mobile node antenna and the anchor node azimuthal antenna faces perfectly facing for every azimuthal antenna of the array, and the path covers the whole azimuthal domain: 100 tracking trials are made, showing that the DoA localization error is systematic and related to the weaknesses in the design of the array structure.

Fig.13 shows a mean detection error $\Delta\varphi < 10^\circ$. In DoAs with $\varphi \in [120^\circ, 180^\circ]$ show a greater local

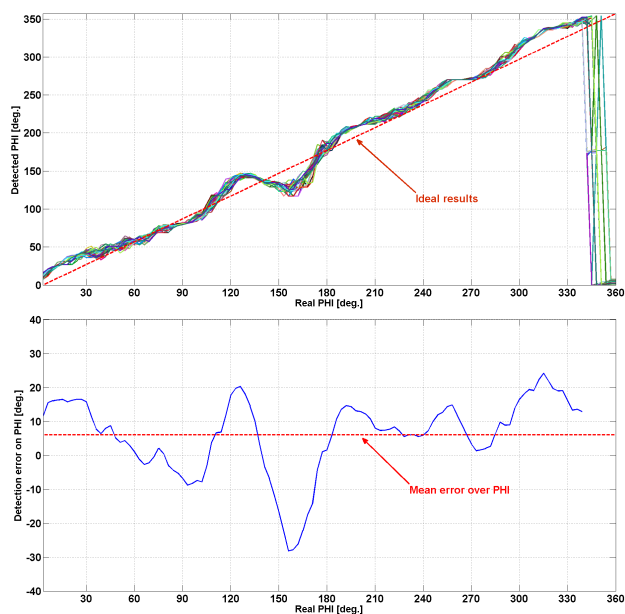


Figure 13: Localization tracking for $\theta = 54^\circ, \phi = 0^\circ \dots 360^\circ$ over 100 trials: tracking results (a) tracking mean error (b)

error ($\Delta\varphi \in [-20^\circ, 20^\circ]$) that is due to the antenna's real pattern deviation from the ideal reference model (used as reference map) as shown in Fig. 12b. This figure also shows the reduced dispersion between the DoA localization results for different tracking trials: for every DoA, the standard deviation is smaller than 10° , so the algorithm's robustness to RSSI deviations due to radio channel noise (basically minimized by IEEE compliant RSSI detection) and to direct detection error is proven.

5 Conclusions

The paper has shown how, using an adapted MUSIC algorithm, it is possible to achieve a good accurate positioning adopting only RSSI estimations without the need of channel propagation parameter estimation (as opposed to [1]), using cost-effective hardware, and maintaining the desirable standard IEEE network compatibility and integrability (as suggested in [15]). The availability of individual anchor nodes capable of self-consistent DoA localization permits reducing the number of anchor points on site (as opposed to [1]) because every anchor node can provide a processed and de-noised positioning information, that is further processed together with all the other positioning information of the anchor nodes, thus giving two different levels of information refining.

The reported experimental results are intended for a single anchor DoA-only localization system: while

it is mandatory to use multiple anchors to give a complete 3-dimensional localization of nodes (with triangulation-like approaches), the accuracy can be further increased including some mobile node side motion tracking systems (such as IMUs, as in [16]). It is clear that a hardware system like that in [11] combined with improved data processing algorithm herein presented, become an effective solution to solve coarse sub-metre positioning in an indoor environment.

References:

- [1] F. Ileri, M. Akar, *RSSI Based Position Estimation in ZigBee Sensor Networks*, WSEAS Recent Advances in Circuits, Systems, Signal Processing and Communications, 2014, pp.62–73
- [2] M. Helen, J. Latvala, H. Ikonen and J. Niitty-lahti, *Using Calibration in RSSI-based Location Tracking System*, WSEAS Proc. of the 5th World Multiconference on Circuits, Systems, Communications and Computers, Jul. 2001
- [3] Ralph O. Schmidt, *Multiple Emitter Location and Signal Parameter Estimation*, IEEE transaction on Antennas and propagation 1986, n.3, vol.AP-34, pp.276–280
- [4] P. Stoica and A. Nehorai, *MUSIC, Maximum Likelihood, and Cramer-Rao Bound*, IEEE transaction on Acoustics, speech and signal processing 1989, n.5, vol.37, pp.720–741
- [5] A.K. Cline and I.S. Dhillon, *Computation of the Singular Value Decomposition*, Handbook of Linear Algebra 2006
- [6] G. Giorgetti, S. Maddio, A. Cidronali, S.K.S. Gupta and G. Manes, *Switched beam antenna design principles for Angle of Arrival estimation*, 2nd European Wireless Technology Conference 2009, n.8, vol.5, pp.5–8
- [7] S. Maddio, A. Cidronali, I. Magrini and G. Manes, *A design method for single-feed wideband microstrip patch antenna for switchable circular polarization*, European Microwave Conference 2007, pp.262–265
- [8] S. Maddio, A. Cidronali and G. Manes, *A New Design Method for Single-Feed Circular Polarization Microstrip Antenna With an Arbitrary Impedance Matching Condition*, Antennas and Propagation, IEEE Transactions on 2011, n.2, vol.59, pp.379–389
- [9] A. Cidronali, S. Maddio, G. Giorgetti, I. Magrini, S.K.S. Gupta and G. Manes, *A 2.45*

GHz Smart Antenna for Location-Aware Single-Anchor Indoor Applications, Microwave Symposium Digest (MTT) 2009, 7-12 June, pp.1553–1556

- [10] A. Cidronali, S. Maddio, G. Giorgetti and G. Manes, *Analysis and Performance of a Smart Antenna for 2.45-GHz Single-Anchor Indoor Positioning*, *IEEE transaction on Microwave Theory Techniques* 2010, n.1, vol.58, pp.21–31
- [11] S. Maddio, M. Passafiume, A. Cidronali and G. Manes, *A Scalable Distributed Positioning System Augmenting WiFi Technology*, *Proceedings of International Conference on Indoor Positioning and Indoor Navigation (IPIN)* 2013, pp.733–742
- [12] S. Maddio, M. Passafiume, A. Cidronali and G. Manes, *Impact of the Dihedral Angle of Switched Beam Antennas in Indoor Positioning based on RSSI*, *Wireless Technology Conference, EuMC* 2014, in press
- [13] *CC2430 datasheet*, *Texas Instrument/Chipcon Products Datasheets* 2012
- [14] *Wireless LAN Medium Access Control (MAC) and Physical Layer (PHY) Specifications*, *IEEE Standard for Information technology, Telecommunications and information exchange between systems, Local and metropolitan area networks, Specific requirements* 2007, 12 Jun., Part 11
- [15] S. Fuicu, M. Marcu, B. Stratulat and A. Girban, *Effectiveness and accuracy of wireless positioning systems*, *WSEAS Transactions on Computers* 8, 2009, no.9, pp.1471–1483
- [16] D. Ofrim, D. Sacaleanu, R. Stoian and V. Lazarescu, *A 3-dimensional Localization Algorithm for Mobile Wireless Multimedia Sensor Networks*, *NAUN International Journal of Communications*, 2011, issue 4, vol.5, pp.149–156